Immunization with a Chimera Consisting of the B Subunit of Shiga Toxin Type 2 and Brucella Lumazine Synthase Confers Total Protection against Shiga Toxins in Mice

María P. Mejias, Giselle Ghersi, Patricio O. Craig, Cecilia A. Panek, Leticia V. Bentancor, Ariela Baschkier, Fernando A. Goldbaum, Vanesa Zylberman and Marina S. Palermo

J Immunol 2013; 191:2403-2411; Prepublished online 5 August 2013;
doi: 10.4049/jimmunol.1300999
http://www.jimmunol.org/content/191/5/2403

The Journal of Immunology is published twice each month by
The American Association of Immunologists, Inc.,
9650 Rockville Pike, Bethesda, MD 20814-3994.

Print ISSN: 0022-1767 Online ISSN: 1550-6606.

Immunization with a Chimera Consisting of the B Subunit of Shiga Toxin Type 2 and Brucella Lumazine Synthase Confers Total Protection against Shiga Toxins in Mice

María P. Mejias,* Giselle Ghersi,† Patricio O. Craig,‡ Cecilia A. Panek,* Leticia V. Bentancor,* Ariela Baschkier,§ Fernando A. Goldbaum,†,‡ Vanesa Zylberman,†,‡ and Marina S. Palermo*

The striking feature of enterohemorrhagic *Escherichia coli* (EHEC) infections is the production of Shiga toxins (Stx) implicated in the development of the life-threatening hemolytic uremic syndrome. Despite the magnitude of the social impact of EHEC infections, no licensed vaccine or effective therapy is available for human use. One of the biggest challenges is to develop an effective and safe immunogen to ensure nontoxicity, as well as a strong input to the immune system to induce long-lasting, high-affinity Abs with anti-Stx–neutralizing capacity. The enzyme lumazine synthase from *Brucella* spp. (BLS) is a highly stable dimer of pentamers and a scaffold with enormous plasticity on which to display foreign Ags. Taking into account the advantages of BLS and the potential capacity of the B subunit of Stx2 to induce Abs that prevent Stx2 toxicity by blocking its entrance into the host cells, we engineered a new immunogen by inserting the B subunit of Stx2 at the amino termini of BLS. The resulting chimera demonstrated a strong capacity to induce a long-lasting humoral immune response in mice. The chimera induced Abs with high neutralizing capacity for Stx2 and its variants. Moreover, immunized mice were completely protected against i.v. Stx2 challenge, and weaned mice receiving an oral challenge with EHEC were completely protected by the transference of immune sera. We conclude that this novel immunogen represents a promising candidate for vaccine or Ab development with preventive or therapeutic ends, for use in hemolytic uremic syndrome–endemic areas or during future outbreaks caused by pathogenic strains of Stx-producing *E. coli*. *The Journal of Immunology*, 2013, 191: 2403–2411.

Enterohemorrhagic *Escherichia coli* (EHEC) strains are important human food-borne pathogens (1). The clinical manifestations of EHEC infections range from watery diarrhea, or hemorrhagic colitis, to the most severe outcome, the life-threatening hemolytic uremic syndrome (HUS) (2). The infection correlates with ingestion of contaminated meat or vegetables, but it is also transmitted by water or even person-to-person contact (3, 4). Sporadic or massive outbreaks have been reported in several developed countries; however, in Argentina, HUS shows an endemic behavior and represents a serious public health problem with high morbidity and mortality (5, 6).

The striking feature of EHEC infection is the production of potent Shiga toxins (Stx), which are responsible for HUS development (7, 8). Stx are formed by a single A subunit, which possesses *N*-glycosidase activity to the 28S rRNA and promotes protein synthesis inhibition in eukaryotic cells, and five B subunits, which bind to globotriaosylceramide (Gb3Cer) at the surface of host cells (9, 10). Although two major types (Stx1 and Stx2) and several subtypes (variants) have been described, Stx2 and its variant Stx2c are the toxins found most frequently in severe HUS cases among EHEC-infected subjects (11, 12). Stx1 and Stx2 differ significantly both in amino acid sequences and in biological functions (13, 14). Although some investigators (15–17) reported that Stx1 and Stx2 do not provide heterologous protection through their B subunits, this matter remains controversial. In contrast, Stx2c and Stx2d variants are readily neutralized with Abs against Stx2 but not with Abs against Stx1 (18). Despite the magnitude of the social and economic problems caused by EHEC infections, no licensed vaccine or effective therapy is available for human use. One of the biggest challenges is to develop an effective and safe immunogen to ensure nontoxicity, as well as a strong input to the host immune system to induce long-lasting, high-affinity Abs that ensure a good neutralization capacity in serum. Despite multiple approaches, this goal has not been reached, primarily because the B subunit of Stx2 (Stx2B), one of the most attractive candidates, is a very poor immunogen (19). It is known that there is a close correlation between the degree of repetitiveness and thermodynamic stability of an Ag and the efficiency of induction of the B cell response (20). Several studies showed that the pentameric arrangement of Stx2B is only marginally stable (21), explaining,

*Laboratorio de Patogénesis e Inmunología de Procesos Infecciosos, Instituto de Medicina Experimental, Consejo Nacional de Investigaciones Cientificas y Tecnicas, Academia Nacional de Medicina, Buenos Aires C1425AUM, Argentina; †INMUNOVA S. A., Buenos Aires C1405BWE, Argentina; ‡Fundación Instituto Leloir, Instituto de Investigaciones Bioquímicas de Buenos Aires – Consejo Nacional de Investigaciones Cientificas y Tecnicas, Buenos Aires C1405BWE, Argentina; and §Servicio de Fisiopatogenia, Instituto Nacional de Enfermedades Infecciosas – Administración Nacional de Laboratorios e Institutos de Salud "Dr. Carlos G. Malbrán," Buenos Aires 1281, Argentina

Received for publication April 12, 2013. Accepted for publication July 1, 2013.

This work was supported by grants from Consejo Nacional de Investigaciones Cientificas y Tecnicas and Agencia Nacional de Promoción Científica y Tecnológica, Argentina.

Address correspondence and reprint requests to Dr. Marina S. Palermo, Instituto de Medicina Experimental, Consejo Nacional de Investigaciones Cientificas y Tecnicas, Academia Nacional de Medicina, Pacheco de Melo 3081, Buenos Aires C1425AUM, Argentina. E-mail address: mspalermo@hematologia.anm.edu.ar

The online version of this article contains supplemental material.

Abbreviations used in this article: AH, aluminum hydroxide; BLS, lumazine synthase from *Brucella* spp.; CD, circular dichroism; EHEC, enterohemorrhagic *Escherichia coli*; FA, Freund's adjuvant; Gb3Cer, globotriaosylceramide; HUS, hemolytic uremic syndrome; LD_{100}, 100% lethal dose; N/A, no adjuvant; rStx1, recombinant Shiga toxin 1; rStx2, recombinant Shiga toxin 2; SLS, static light scattering at 90°; Stx, Shiga toxin; Stx2B, B subunit of Shiga toxin 2; TSB, Tryptic Soy Broth.

at least in part, its lack of immunogenicity. The enzyme lumazine synthase from *Brucella* spp. (BLS) is a highly immunogenic and stable dimer of pentamers and a scaffold with enormous plasticity on which to display foreign Ags (22–26). The N terminal of each monomer would be displayed at the vertices of a symmetric pentamer at a distance of 40 Å. These are the insertion sites that we used to decorate BLS with Stx2B, taking advantage of the similarity of the oligomeric state of both proteins. We reasoned that BLS would be a perfect scaffold to accommodate and stabilize the five monomers of the B subunit, as long as a flexible linker long enough to avoid steric hindrance is used to connect the monomers of both proteins. The pentamer of B subunits folded on top of each of the BLS pentamers would benefit from the high local concentration of the subunits dictated by the covalent attachment to the scaffold, as well as the high thermodynamic stability of BLS. Effectively, the resulting chimera (BLS-Stx2B) showed a remarkable stability and demonstrated a strong capacity to induce long-lasting humoral immune responses. The chimera administered to mice under different formulations and regimens induced Abs with a high neutralizing capacity for Stx2 and its variants. Moreover, mice immunized with BLS-Stx2B were completely protected against challenges with high lethal doses of Stx2 up to 10 mo after the last immunization. Most importantly, sera from immunized mice also protected mice during a relevant model of EHEC infection, demonstrating that the transferred Abs were capable of neutralizing the toxin as it is delivered by EHEC. We conclude that this novel immunogen represents a promising candidate for vaccine or Ab development, with preventive or therapeutic purposes to be used in HUS-endemic areas or during future outbreaks caused by pathogenic strains of Shiga toxin–producing *E. coli*.

Materials and Methods

Ethics statement

Experiments were approved by the Instituto de Medicina Experimental Care Committee in accordance with the principles set forth in the National Institutes of Health's *Guide for the Care and Use of Laboratory Animals*.

Molecular modeling

The theoretical structure of the BLS-Stx2B chimera was modeled with the program PyMOL 1.5 (http://www.pymol.org), fusing the C-terminal end of the structure of Stx2B (PDB code: IR4P) with the N-terminal end of the crystallographic structure of BLS (PDB code: IDI0) through a decapeptide linker of sequence GSGSGSGSGS.

Engineering, expression, and purification of BLS-Stx2B

The Stx2B-coding sequence was amplified by PCR with primers Forward 5′-ATCAACATGCATGCGGATTGTGCTAAAGGT-3′ (NsiI site underlined) and Reverse10 5′-TAAAATCTTAAG**AGAACCAGAACCAGAACCAGAACCAGAACC**GTCATTATTAAACTGCAC-3′ (AflII site underlined). Primer Reverse10 included the coding sequence for a 10-aa linker (bold type). The PCR product was cloned upstream to the BLS gene, in a pET11a vector that was generated previously and contains the BLS sequence (26), generating plasmid pET-BLS-Stx2B. To ensure that the plasmid construct was intact and functional, it was sequenced across the gene insert.

The plasmid was transformed into *E. coli* BL21 (DE3)-competent cells for expression of the recombinant protein. Inclusion bodies containing BLS-Stx2B were solubilized by overnight incubation in 8 M urea, 50 mM Tris/HCl, 5 mM EDTA (pH 8) buffer and dialyzed against 1 M urea, 50 mM Tris/HCl, 5 mM EDTA (pH 8.5) buffer. The solubilized proteins were purified by anion exchange chromatography in a Q-Sepharose column (Pharmacia, GE Healthcare Life Sciences) using an HPLC apparatus (Gilson model 320). Elution was performed using a linear gradient between 0 and 1 M NaCl in buffer consisting of 1 M urea and 50 mM Tris/HCl (pH 8.5).

Protein was dialyzed against PBS prior to each immunization.

pCI-BLS-Stx2B DNA vaccine

To develop a DNA vaccine coding for BLS-Stx2B (pCI-BLS-Stx2B), the BLS-Stx2B DNA sequence was amplified by PCR, using pET-BLS-Stx2B as a template, and subcloned in the pCI-neo vector (Promega, Madison, WI), with primers pCI Forward 5′-GTTTAA**GAATTC**GAAGGAGATACC**ACCATG**CATGCGGAT-3′ (EcoRI site underlined; KOZAK consensus sequence in bold type) and pCI Reverse 5′-TGTCCACCAGTCATGCTAGCTCAGACAAGCGCGATGC-3′ (NheI site underlined). To ensure that the plasmid construct was intact and functional, it was sequenced across the gene insert.

Plasmid was amplified in *E. coli* DH5α cells and isolated using Maxiprep plasmid isolation columns (QIAGEN, Valencia, CA), following the manufacturer's instructions.

Proteins used in this study

BLS and Stx2B. BLS and Stx2B were expressed and purified, as previously described (26, 27). Briefly, BLS was purified in a Mono-Q column in an HPLC apparatus using a linear gradient of NaCl between 0 and 1 M in 50 mM Tris (pH 8.5) buffer. The peak enriched with BLS was further purified on a Superdex-200 column with PBS and 1 mM DTT. Stx2B was purified by affinity chromatography under native conditions with Ni-NTA resin (QIAGEN), following the manufacturer's instructions. The purity of the preparation was determined on SDS-PAGE 15% (w/v) polyacrylamide gels.

Crude preparation of recombinant Stx2 and purified recombinant Stx1. Recombinant plasmids for expression of recombinant Stx2 (rStx2) and recombinant Stx1 (rStx1) were generated previously (28, 29). The culture of recombinant *E. coli* JM109 strain, transformed with the recombinant plasmid pGEM-Stx2 or pGEM-Stx1, was obtained by overnight incubation in Luria–Bertani broth supplemented with ampicillin. Bacterial cells were centrifuged, and the resultant pellet was resuspended in PBS with 1 mM PMSF and lysed by sonication. To obtain the crude preparation of rStx2, the lysate from JM109/pGEM-Stx2 was centrifuged (14,000 rpm, 20 min 4°C), and the supernatant was precipitated with ammonium sulfate solution (75%). The pellet was resuspended in PBS, dialyzed against the same buffer for 24 h, and stored at −20°C until use. Total protein concentration was determined using standard methods. Stx2 concentration was determined with a RIDASCREEN Verotoxin kit (R-BIOPHARM, Darmstadt, Germany) (30, 31). rStx1 was purified by affinity chromatography with commercially available Globotriose Fractogel (IsoSep, Tullinge, Sweden), as previously described (30). Briefly, the supernatant from JM109/pGEM-Stx1 was applied to the Globotriose Fractogel column and incubated at 4°C for 2 h. rStx1 was eluted with PBS containing 4 M $MgCl_2$. The eluted material was pooled, dialyzed against PBS, and concentrated by centrifugation filtration with a 5000 MWCO Amicon Ultra concentration system (Millipore). The purity of the preparation was determined by SDS-PAGE (15%, w/v) and quantified by standard methods.

Stx2-producing EHEC. Stx2-producing EHEC and Stx2 variants were generously provided by Dr. Marta Rivas (Administración Nacional de Laboratorios e Institutos de Salud "Dr. Carlos G. Malbrán"). *E. coli* 680/01 (O157:H7, produces Stx2), *E. coli* 242/01 (O174:H21, produces Stx2c), and *E. coli* 265/02 (O171:H2, produces Stx2d) were grown overnight. Cultures were centrifuged at 15,000 × *g* for 20 min at 4°C, and supernatants were collected and stored at −20°C until used.

Structural analysis of BLS-Stx2B

Circular dichroism. The circular dichroism (CD) spectra of BLS-Stx2B, BLS, and Stx2B in the far UV region (255–200 nm) were measured on a JASCO J-810 spectropolarimeter in PBS (pH 7) buffer at 25°C, using quartz cuvettes of either 1- or 5-mm path length. Data were converted to molar ellipticity [θ]/dmol protein (deg cm^2 $dmol_{prot}^{-1}$).

Static light scattering. The average molecular mass of BLS-Stx2B was determined on a Precision Detectors PD2010 light scattering instrument connected in tandem to an HPLC system, including a Waters 486 UV detector and an LKB 2142 differential refractometer. Proteins were run on a Superdex 200 column (Amersham Biosciences, Uppsala, Sweden) and eluted in PBS, 1 M urea (pH 7) buffer. The elution was monitored by measuring the static light scattering at 90° (SLS), the UV absorption at 280 nm, and the refractive index signals. The data were recorded on a PC computer and analyzed with Discovery32 software supplied by Precision Detectors. The molecular mass was calculated by analysis of the SLS and refractive index signals and comparison of the results with the ones obtained for BSA as standard (molecular mass 66.5 kDa).

Gb3Cer-binding assay. The assay was performed as previously described (32). Gb3Cer (Matreya, State College, PA) dissolved in chloroform/methanol (2:1) was used to coat 96-well ELISA plates (Greiner Bio-One, Frickenhausen, Germany) at 1 μg/well. A pool of sera from BLS-Stx2B–immunized mice was used as primary Ab (diluted 1:1000), and peroxidase-conjugated goat anti-mouse IgG (Zymed; Invitrogen, Carlsbad, CA) was used as secondary Ab (dilution 1:3000). The reaction was developed with

O-phenylenediamine (Sigma, St Louis, MO), and absorbance was read at 492 nm. BLS and *E. coli* BL21 extracts were used as negative controls for nonspecific binding.

Immunization protocols and sample collection

Adult BALB/c mice (2 mo old) were immunized with three doses of BLS-Stx2B: i.p. with Freund's adjuvant (FA; DIFCO-BD, Detroit, MI), s.c. with aluminum hydroxide (AH), or i.p. with no adjuvant (N/A) on days 0, 15, and 30. Groups of mice also were immunized i.p. with BLS and Stx2B in FA. The doses of BLS and BLS-Stx2B were corrected by their molecular weights to inoculate equimolar amounts of each protein compared with that of Stx2B (the dose was equivalent to 20 μg Stx2B).

For prime boost immunization, mice were injected i.m. with 100 μg pCI-BLS-Stx2B on days 0, 14, and 28 into the rear legs, followed by a final i.p. booster of BLS-Stx2B in incomplete FA at day 40.

Analysis of Ab responses

Stx2B-specific IgG determination. ELISA plates were coated with 0.5 μg/well Stx2B. For total specific IgG determination or IgG subtyping, peroxidase-conjugated goat anti-mouse IgG or IgG1 and IgG2a (1:1000; BD Pharmingen, Franklin Lakes, NJ) were used as secondary Abs. The Ag–Ab reaction was detected as described for the Gb3Cer-binding assay. Results were expressed as end point titers, calculated as the reciprocal values of the last dilution with an OD higher than that of the preimmune serum samples ± 2 SD.

Ab-affinity determination. The Stx2B affinities of Abs raised in immunized mice were determined by the thiocyanate elution–based ELISA, as previously described (33). The concentration of ammonium thiocyanate required to dissociate 50% of the bound Ab was determined. The percentage of binding was calculated as follows: OD_{492nm} in the presence of ammonium thiocyanate × 100/OD_{492nm} in the absence of ammonium thiocyanate.

In vitro and in vivo neutralizing activity. Stx2-neutralizing Ab titers were determined as previously described (18), with 1 CD_{50} of rStx2 (670 pg Stx2). The neutralizing activity was expressed as the reciprocal value of the highest dilution that blocked 50% of Stx2 toxicity to Vero cells. The same assay was performed using purified rStx1 or supernatants from EHEC strains producing Stx2, Stx2c, or Stx2d (1 CD_{50}/well).

For the ex vivo assay, 2.2 ng/mouse of rStx2 (one 100% lethal dose; 1 LD_{100}) was preincubated with sera from immunized and nonimmunized mice for 1 h at 37°C and 1 h at 4°C. The mixture was inoculated i.v. into naive adult BALB/c mice, and survival was observed.

Finally, immunized mice were challenged by i.v. inoculation with 1 LD_{100} rStx2 50 d after the last immunization. Surviving mice were rechallenged with 3 LD_{100} (6.6 ng/mice) 10 mo after the last dose.

Analysis of Ab efficacy against EHEC challenge

Bacterial strain and growth. The enterohemorrhagic Stx2-producing *E. coli* O157:H7 (EHEC) was isolated from a fecal specimen of a child with HUS and was characterized by Brando et al. (34). Bacterial cultures were performed as previously described (34). Briefly, strains were cultured overnight at 37°C in Tryptic Soy Broth (TSB) (Difco, Le Point de Claix, France). A 250-ml volume was inoculated into five Erlenmeyer flasks (125 ml) containing 25 ml TSB and incubated at 37°C for 18 h. Cultures were centrifuged, and bacterial pellets were washed twice in PBS and then resuspended in 1 ml PBS. Aliquots were diluted (10^2–10^4), plated onto Plate Count Agar, and incubated overnight at 37°C. Overnight cultures reached a final concentration of 1–1.8 × 10^{10} CFU/ml. The strain was maintained at −70°C in TSB supplemented with 20% glycerol.

Mice and oral infection. Immature male and female BALB/c mice were used immediately after weaning (17–19 d of age, ~8–11 g body weight). Weaned mice were divided randomly into experimental groups. After 8 h of starvation (35, 36), animals were inoculated i.p. with 50 μl nonimmune or immune sera (BLS-Stx2B+FA, 45 d post last immunization, diluted 1:100 in PBS) and intragastrically inoculated via a stainless steel cannula (0.38 mm × 22G) (model 7.7.1; Harvard Apparatus, Holliston, MA) with 0.1 ml bacterial suspension (4 × 10^{11} CFU/kg). Food and water were provided to mice ad libitum 4 h after the ingestion of the bacterial suspension.

Analysis of EHEC pathogenicity. Blood samples were obtained at 48 and 72 h after bacterial feeding for laboratory analyses that included total and differential blood cell count in a Neubauer chamber and blood urea nitrogen determination. Biochemical determinations of urea in mouse plasma were performed in an autoanalyzer CCX spectrum (Abbot Diagnostics Systems, Buenos Aires, Argentina), following standardized instructions.

Rectal swabs were taken at 72 h postinfection to determine the excretion of *E. coli* O157:H7 bacteria. These samples were cultured onto sorbitol MacConkey agar (Difco) at 37°C for 18 h. The nonfermenting sorbitol colonies in confluent growth zones were screened for *stx1*, *stx2*, and *rfbO157* genes by a multiplex PCR using the primers described by Leotta et al. (37), Ziebell et al. (38), and Paton and Paton (39), respectively. The reference *E. coli* strains EDL933 O157:H7 (*stx1* and *stx2*) and ATCC 25922 were used as positive and negative controls of gene expression, respectively.

Statistical analysis

Data are presented as the mean ± SEM of each group of mice. Statistical differences were determined using one-way multiple-comparison ANOVA by the ANOVA–Newman–Keuls Test, and $p < 0.05$ was considered significant. Comparisons between two groups were performed with the Student *t* test. The log-rank test was used to compare survival curves. The *p* values < 0.05 were considered significant.

Results

Engineering of the chimeric protein BLS-Stx2B

The construction of the chimera was carried out using the strategy described by Laplagne et al. (26). The coding sequence of the first eight residues of the N-terminal end of BLS was replaced with the coding sequence of Stx2B and a flexible G/S decapeptide linker (GSGSGSGSGS) that connects both proteins. Both Stx2B and BLS form pentameric structures of the same C5 symmetry in which each protomer interacts with the other two. Molecular modeling of the chimera (Fig. 1) suggests that the linker used would be long enough to allow assembly of the Stx2B pentamers onto the pentameric modules of BLS without any steric hindrance. In the decameric BLS particle, two Stx2B pentamers are displayed in opposite directions at the top and bottom of the structure. It is worth noting that, in the BLS-Stx2B chimera, the Gb3Cer-binding surface of Stx2B is totally exposed to the solvent and is distal to the BLS scaffold.

Expression and characterization of recombinant BLS-Stx2B protein

The plasmid pET-BLS-Stx2B was transformed into competent *E. coli* BL21 (DE3) cells. The inclusion bodies, containing the majority of the BLS-Stx2B protein, were dissolved in 8 M urea. Because wild-type BLS remains folded in those conditions (23,

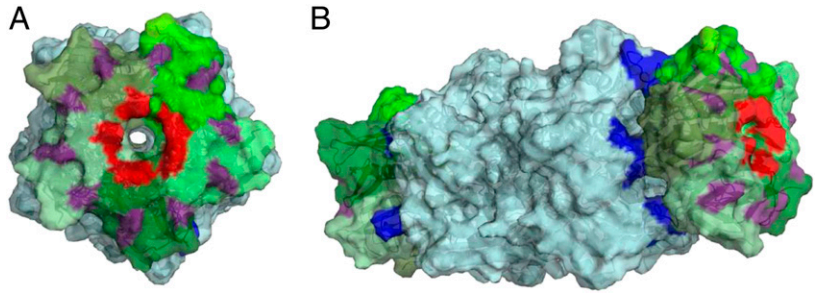

FIGURE 1. Molecular modeling of BLS-Stx2B. (**A**) Top view of BLS-Stx2B. Stx2B pentamer was assembled on top of the BLS pentamer without steric hindrance. Each Stx2B pentamer is a different shade of green, and the BLS decamer is cyan. The flexible decapeptide linker is blue. Four amino acids from binding site 1, which requires the pentameric assembly of Stx2B for binding to Gb3Cer, are magenta: Trp29, Glu15, Gly60 (relevant for toxicity), and Glu64 (from adjacent monomer). Trp34 from binding site 3 is red. These amino acids were colored to highlight the importance of the pentameric assembly achieved in BLS-Stx2B. (**B**) Lateral view of BLS-Stx2B.

40, 41), we reasoned that, in 8 M urea, the chimera would have BLS in the folded state, whereas the Stx2B subunit would be in the unfolded state. Thus, we decided to dialyze the protein against 1 M urea to allow refolding of Stx2B and the correct assembly of the protein particle. The refolded material was purified by ionic-exchange chromatography (Supplemental Fig. 1).

SLS and CD analyses were performed to confirm the correct folding of the BLS-Stx2B protein. In the size-exclusion chromatography coupled to SLS analysis, the agreement between the theoretical molecular mass (254 kDa) and the molecular mass observed for the major peak (234 kDa) (Fig. 2A) indicates that BLS folds as a decamer in the chimera. In addition, we observed a first peak at the void volume of the column, corresponding to higher molecular mass aggregates of this protein. The far UV-CD spectrum of BLS-Stx2B (Fig. 2B) was shown to be nearly identical to that theoretically calculated for this protein from the combination of the CD signals of the isolated BLS and Stx2B modules. Altogether, these results indicate that both BLS and Stx2B are properly folded in the structure of the chimera and that BLS-Stx2B has the expected quaternary structure.

Binding of BLS-Stx2B to Gb3Cer

Because the pentameric conformation of Stx2B is required for Gb3Cer binding, a Gb3Cer-binding ELISA assay was used to functionally confirm that BLS-Stx2B assembled into the native holotoxin B subunit configuration. We observed a positive reaction in a dose-dependent fashion with the chimera and the rStx2 holotoxin but not with BLS (Fig. 2C). Because the primary Ab used in the ELISA was a pool of sera from BLS-Stx2B–immunized mice, OD values did not allow us to draw conclusions about differences in the avidity for Gb3Cer between the different ligands. However, it allowed us to confirm that the binding of BLS-Stx2B to Gb3Cer was mediated through Stx2B and not through unspecific binding of BLS. From these findings, we conclude that the B subunits on top of the BLS decamer are correctly assembled and maintain their Gb3Cer-binding capacity.

Analysis of the immune response

Time course of the Ab titers during the immunization. To assess the ability of BLS-Stx2B to improve the humoral immune response compared with the isolated recombinant purified Stx2B subunit, groups of mice were injected i.p. with equimolar amounts of the chimera or Stx2B in the presence of FA. We examined specific IgG Ab in sera from vaccinated mice for >2 mo. IgG Abs specific to Stx2B were elicited in both vaccinated groups (Fig. 3). ELISA titers of the BLS-Stx2B group increased during the first three vaccinations and peaked at 14 d after the third vaccination. However, Stx2B-immunized mice did not show a specific Ab response before 45 d after the first vaccination, with high titer variability between individuals. At all analyzed times, the Ab titers generated by BLS-Stx2B were significantly higher than those of the Stx2B group ($p < 0.005$) (Fig. 3). No Stx2B-specific Abs were detected in the BLS-immunized group.

Ab titers under different immunization protocols. To evaluate the capacity of BLS-Stx2B to stimulate the immune system and to generate Abs under different formulations or vaccine regimens, we immunized groups of mice with BLS-Stx2B protein with FA or AH, without any adjuvant, or following a DNA–protein prime-boost schedule. Serum samples were collected at different times after vaccination, and titers of specific IgG were determined by ELISA. The results indicate that BLS-Stx2B stimulates the immune response under all protocols tested, even without any exogenous adjuvant (Fig. 3). However, differences in the intensity and/or kinetics of the humoral response among different protocols were observed. In particular, immunization with BLS-Stx2B formulated in AH or FA was kinetically similar in the development of specific Ab, but mice immunized with FA reached significantly higher titers (Fig. 3). In contrast, the DNA–protein prime-boost regimen induced Stx2B-specific Abs later (35 d after the protein boost), but at the same time reached similar titers than BLS-Stx2B with AH. The protein in the absence of adjuvant induced the lowest humoral response, in terms of maximal titers and time needed to reach them. In fact, mice from this group showed anti-Stx2B–specific Abs after the third immunization, and the Ab titer was 10-fold lower than in mice immunized with BLS-Stx2B in AH.

Ab subtyping. IgG1 is associated with the Th2-mediated humoral immune response, and IgG2a is associated with the Th1-mediated cellular response (42). To determine which type dominates the immune response, we examined the titers of the IgG subtypes (IgG1 and IgG2a) in mouse sera from all BLS-Stx2B groups at 45 d after the last immunization. BLS-Stx2B Ag induced higher anti-Stx2B–specific IgG1 titers than IgG2a titers ($p < 0.001$) for all protocols analyzed, with the exception of the prime-boost schedule, in which there was no significant difference between the IgG subclasses (Supplemental Fig. 2).

Ab affinity. Because the neutralizing and protective capacity of sera are closely dependent on the titer, as well as on the affinity of Abs for Stx2, we evaluated sera affinity of the different vaccinated groups by ELISA upon dissociation with ammonium thiocyanate. Results shown in Table I indicate that sera from mice immunized with BLS-Stx2B formulated with FA or AH displayed Abs with higher affinity for Stx2B than did sera from mice immunized with purified Stx2B in FA. Similar affinity results were observed in sera collected from mice immunized with BLS-Stx2B without adjuvant or in prime-boost regimens.

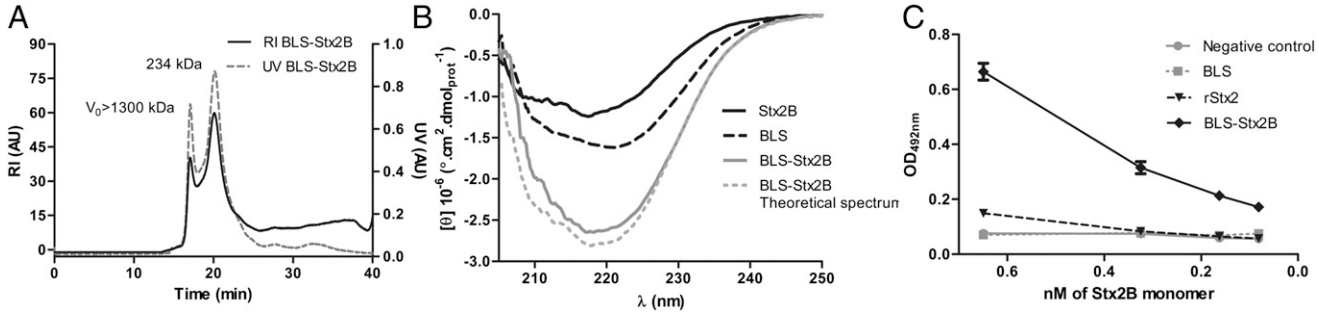

FIGURE 2. Structural analysis of BLS-Stx2B. (**A**) Size-exclusion chromatography coupled to SLS analysis of the BLS-Stx2B chimera. (**B**) Comparison of the far UV-CD spectra of BLS, Stx2B, and BLS-Stx2B. The theoretical spectrum of BLS-Stx2B was calculated from the combination of the Stx2B and BLS spectra. (**C**) Assessment of BLS-Stx2B assembly by the Gb3Cer-binding ELISA assay. Serially diluted BLS-Stx2B, BLS, rStx2, or *E. coli* BL21 lysate (used as negative control for nonspecific binding) was added to Gb3Cer-coated plates. Binding was determined as detailed in *Materials and Methods*.

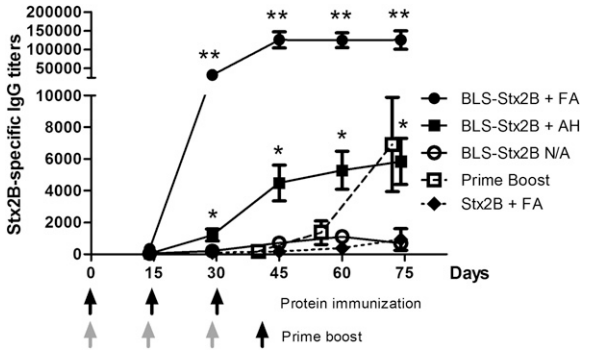

FIGURE 3. Time course of specific IgG titers against Stx2B. Stx2B-specific IgG titers in sera from mice immunized with BLS-Stx2B (in different formulations) or Stx2B (formulated in FA) were determined by ELISA, as detailed in *Materials and Methods*. Each time point represents the mean ± SEM of four to six mice/group. Black arrowheads indicate protein immunizations; gray arrowheads indicate DNA immunizations. Results are representative of two separate experiments. $*p < 0.05$, versus the same time point for BLS-Stx2B N/A and Stx2B + FA groups, $**p < 0.005$, versus the same time point for all others groups.

Neutralization titers against rStx2. A more correlative in vitro indicator of the protective immune response is the neutralizing capacity in the Vero cells' cytotoxicity assay. Sera from mice immunized with BLS-Stx2B formulated with FA showed the highest neutralizing titer in the neutralization test against rStx2 ($p < 0.001$). In contrast, sera from mice immunized with Stx2B, even when formulated in FA, showed the lowest neutralization activity (Table I). Sera from nonimmunized or BLS-immunized mice did not show neutralization activity.

Cross-reactivity of mouse sera. Additionally, we evaluated neutralizing activity against wild-type toxins produced by pathogenic EHEC strains. For this purpose, supernatants from human-isolated EHEC strains producing Stx2 or the Stx2c or Stx2d variant were incubated with sera from immunized mice, and toxicity on Vero cells was evaluated. We also evaluated neutralization capacity against rStx1. Sera from mice immunized with BLS-Stx2B strongly neutralized wild-type Stx2 and its variants, as well as rStx1. In sharp contrast, only the serum sample harvested from one of six mice immunized with Stx2B was able to weakly neutralize wild-type Stx2, and none of them neutralized the Stx2 variants or rStx1 (Table II).

Protection of immunized mice against rStx2 challenge

Ex vivo rStx2-neutralization activity. In addition, anti-Stx2–neutralization activity was evaluated ex vivo in mortality curves by preincubating 1 LD_{100} of rStx2 with one neutralizing unit of each pool of sera from different experimental groups. As indicated in Fig. 4A, preincubation of rStx2 with sera harvested from mice immunized with BLS-Stx2B under all protocols fully abrogated rStx2 toxicity. In contrast, sera collected from mice immunized with Stx2B or BLS did not prevent rStx2 toxicity.

In vivo Stx2-neutralization activity. As a final demonstration of the protective efficacy of the novel BLS-Stx2B vaccine, we challenged all groups of immunized mice with 1 LD_{100} of rStx2 50 d after the last immunization. Fig. 4B shows that 100% of the BLS-Stx2B–vaccinated mice and 33% of the Stx2B-vaccinated mice survived the lethal rStx2 challenge. As expected for 1LD100 of rStx2, 0% of the animals immunized with BLS or that were not immunized survived the challenge (Fig. 4B).

Table I. Ab affinity and rStx2-neutralization capacity of sera from immunized mice

Immunization Protocols	Ab Affinity[a]	Neutralization Titer
BLS-Stx2B + FA	0.87 ± 0.17*	1508 ± 336**
BLS-Stx2B +AH	1.01 ± 0.11*	178 ± 86
BLS-Stx2B N/A	0.52 ± 0.10	104 ± 66
Prime boost	0.62 ± 0.14	203 ± 92
Stx2B + FA	0.41 ± 0.05	60 ± 48

Ab affinity and rStx2-neutralization capacity of mouse sera from immunized mice (45 d post last immunization) were assayed as described in *Materials and Methods*.

Data are mean ± SEM (n = 4–6 mice/group).

[a]Ab affinity is represented as the molar concentration of ammonium thiocyanate required to dissociate 50% of the bound Abs (in ELISA assay).

$*p < 0.05$, versus Stx2B + FA group, $**p < 0.001$, versus all other groups.

Table II. Neutralization titers against purified rStx1, wild-type Stx2, and Stx2 variants

Toxins	BLS-Stx2B + FA	Stx2B + FA
Stx2	2461 ± 522	42 ± 42
Stx2c	1731 ± 346	0
Stx2d	1740 ± 386	0
rStx1	966 ± 486	0

Sera from mice immunized with Stx2B or BLS-Stx2B, both formulated with FA (45 d post last immunization), were incubated in vitro with 1 CD_{50} of rStx1 and EHEC-produced Stx2 variants. Vero cytotoxicity was assayed as detailed in *Materials and Methods*.

Data are mean ± SEM (n = 6 mice/group).

Protection against EHEC pathogenicity

The weaned mouse model is an effective and reliable animal model for studying the pathology of EHEC infection (34, 43). We demonstrated that weaned mice infected with Stx2-producing *E. coli* O157:H7 strains, isolated from HUS patients, experience renal dysfunction and death during the 3 d postinfection. In the same study, we also reported that a similar infection with an O157:H7 strain that does not produce Stx2 did not result in any of the pathological changes seen with the Stx2-producing strain, including a lower intestinal colonization rate. Hence, in this animal model, all of the described pathological changes result from the action of Stx2. For these reasons, we chose the weaned mouse model to assay the capacity of immune sera to protect mice from lethality induced by Stx2 released by EHEC infection in vivo. Naive weaned mice were divided into two groups receiving 50 μl of nonimmune or immune sera (BLS-Stx2B+FA) by i.p. injection immediately before challenge with 4×10^{11} CFU/kg of Stx2-producing *E. coli* O157:H7. Animals were observed daily, and blood and stool samples were collected until death. Fig. 5A shows that mice receiving immune sera were totally protected against death by EHEC infection. Mice receiving nonimmune sera that died after 72 h exhibited high levels of plasmatic urea, indicating renal dysfunction (Fig. 5B), and an increased percentage of circulating neutrophils, as previously described (Fig. 5C) (34). Interestingly, the frequency of O157:H7-positive stool samples, characterized as described in *Materials and Methods*, was higher in mice receiving nonimmune sera compared with those receiving immune sera (Fig. 5D).

Long-term evolution of immune response

Sera from surviving BLS-Stx2B–immunized mice were harvested long-term to study the duration of the specific Ab response (Fig. 6A). Although all BLS-Stx2B regimens induced a long-lasting immune response evaluated as anti-Stx2B Abs by ELISA, the prime-boost regimen was the protocol that induced a level of Ab titers that was the most stable over time, such that anti-Stx2B titers in this group were similar to the FA group at 10 mo after the last immunization. Despite this, all BLS-Stx2B–vaccinated mice survived the challenge with 3 LD_{100} at 10 mo after the last immunization (Fig. 6B).

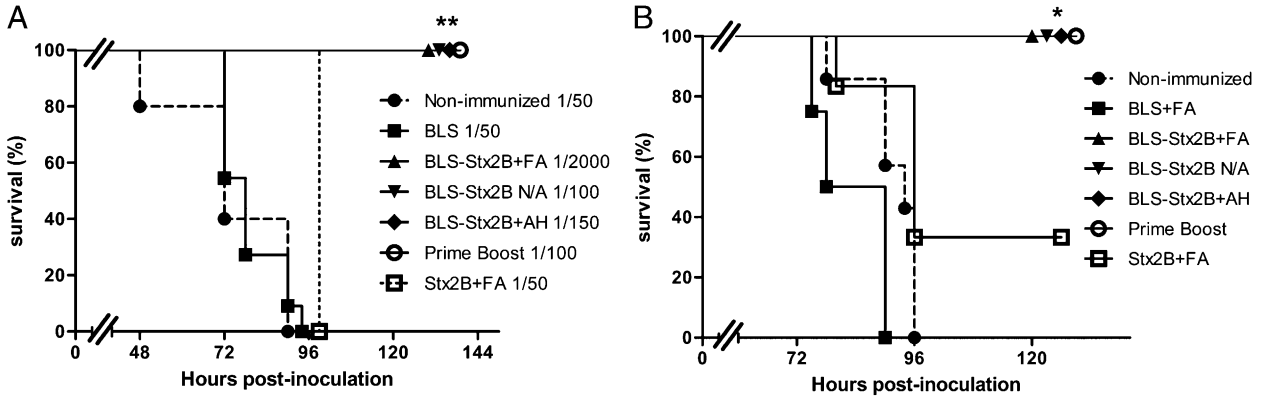

FIGURE 4. Protection of mice against rStx2 toxic activity. (**A**) Ex vivo neutralization of rStx2 toxicity (1 LD_{100}) with sera from immunized mice. Pools of sera from each immunized group (n = 4–6 mice/pool) (45 d post last immunization) or nonimmunized mice were diluted according to the in vitro neutralization titers, as indicated in the key. (**B**) Protection of immunized mice against a lethal challenge of purified rStx2. Mice immunized with Stx2B + FA, different formulations of BLS-Stx2B, or BLS + FA (n = 4–6 mice/group) were challenged i.v. with 1 LD_{100} rStx2 50 d after the last immunization. *$p <$ 0.05, versus Stx2B + FA group, and $p < 0.005$, versus nonimmunized or BLS + FA group, **$p < 0.005$, versus all other groups.

Discussion

The major finding in this study is that a chimera consisting of BLS and Stx2B is highly efficacious as a vaccine against the potent cytotoxins Stx2, Stx2 variants, and Stx1. The use of genetic toxoids of Stx-type toxins is not a novel vaccine strategy (15, 16, 30, 44). However, the genetic construction of a chimeric toxoid engineered with the scaffold protein BLS decorated with 10 units of the B subunit of Stx2 is a new approach to circumvent the lack of immunogenicity of this binding subunit (19).

Both components of the chimeric toxoid were selected based on their particular properties. The B subunit of Stx2 was selected because, among the Stx family, Stx2 is the most pathogenic toxin. Because cross-reactivity between B subunits is controversial (15–17), an Stx2B-based immunogen would protect against the Stx most related to HUS development. In addition, the B subunit represents the binding unit of the toxin and is nontoxic for mammalian cells (9, 10). Abs able to block binding to the specific receptor (Gb3Cer) in mammalian cells should prevent the first step of the toxicity cascade (45). In addition, an Stx-based vaccine against HUS would not only protect against known EHEC strains, typically O157 and non-O157 serotypes, it would also be useful against new or rare pathogenic strains of Stx-producing *E. coli*, such as

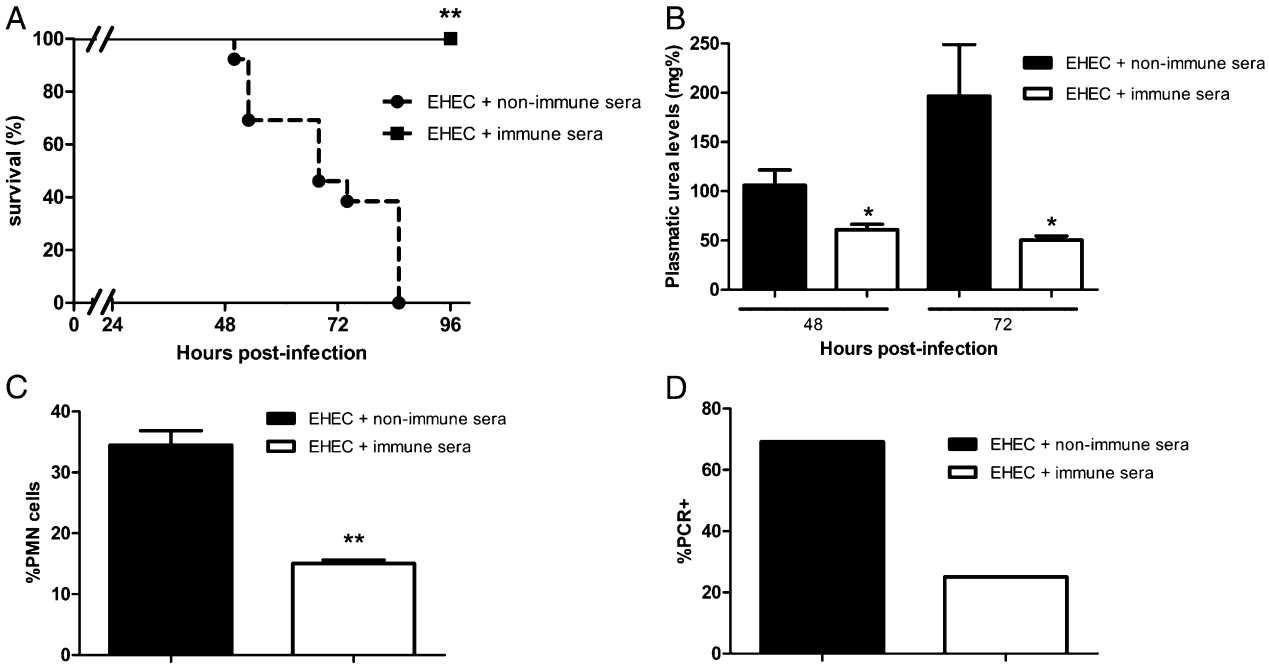

FIGURE 5. Protection against EHEC-induced pathogenicity. (**A**) Protection of weaned mice injected i.p. with immune sera against a lethal intragastric challenge with EHEC. Seventeen- to nineteen-day-old mice (n = 4–10 mice/group) were injected i.p. with 50 μl of nonimmune or immune sera (group BLS-Stx2B + FA, at 45 d post last immunization) diluted 1:100 in PBS. Immediately after injection, mice were infected orally with 4×10^{11} CFU/kg of Stx2-producing *E. coli* O157:H7. Results are representative of two separate experiments. (**B**) Renal Stx2-induced toxicity. Plasmatic urea levels at 48 and 72 h post-EHEC challenge were measured as a correlate of renal damage. Each bar represents the mean ± SEM of 5–10 mice/group. (**C**) Systemic symptoms of HUS-like illness. Mice were bled at 72 h post-EHEC challenge, and total and differential counts of leukocytes were assayed. Each bar represents the mean ± SEM of the relative numbers of PMN cells from four or five mice/group. (**D**) Bacterial shedding in EHEC-infected mice. Fecal samples were obtained at 72 h after challenge (n = 4–13 mice/group). Excretion of *E. coli* O157:H7 was determined by PCR against *Stx2* and *rfbO157* genes in nonsorbitol-fermenting colonies. *$p <$ 0.05, versus nonimmune sera group from the same time point, **$p < 0.005$, versus nonimmune sera group.

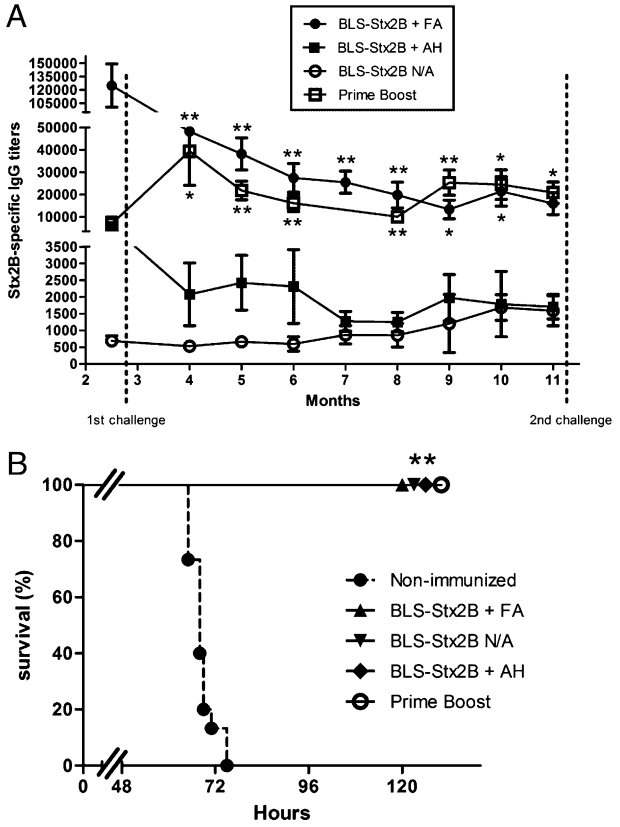

FIGURE 6. Long-term specific IgG Ab response and protective immune response. (**A**) Titers of specific IgG against Stx2B assayed by ELISA up to 10 mo after the last immunization. Each time point represents the mean ± SEM of n = 4–6 mice/group. *$p < 0.05$, **$p < 0.005$, compared with BLS-Stx2B N/A- or AH-immunized mice. (**B**) Mice surviving the first rStx2 challenge received a second challenge with 3 LD_{100} of rStx2 at the time indicated in (A) (second challenge). **$p < 0.005$, versus nonimmunized mice.

the recent large outbreak of HUS caused by the O104:H4 strain (46, 47).

The other component of the chimera, BLS, was chosen because of its advantages as a carrier for Ag delivery (24–26). BLS is especially useful because it folds as a dimer of pentamers that share the same C5 symmetry as the pentameric Stx2B Ag. The N termini of the pentameric modules of BLS are located at opposite sites: at the top and bottom of the decameric particle. These are suitable insertion sites for the display of target proteins through recombinant fusion. However, the display of nonmonomeric proteins in the context of BLS may be problematic because of interparticle cross-linking and aggregation through homomeric interactions of the target subunits. This phenomenon may be critical when protomers remain free because of uneven stoichiometry between the target oligomer and BLS. In contrast, we reasoned that BLS would represent a perfect scaffold for the assembly and stabilization of a pentameric protein if flexible peptide linkers of convenient length are used for the attachment of both proteins to avoid steric hindrance. The results presented in this article indicate that attachment of the Stx2B subunits to the BLS scaffold promotes the pentamerization of the toxin and stabilizes its structure as a result of the high local concentration of the subunits and the influence of the high thermodynamic stability of BLS.

The strong B cell response elicited when mice were immunized with BLS-Stx2B could be explained by this stabilization, as well as by the ability of BLS to target and activate dendritic cells (48). Specific ELISA titers and neutralization activity of the Abs elicited by BLS-Stx2B were improved significantly compared with those elicited by Stx2B when both immunogens were administered in FA. The most likely explanation is that the Stx2B pentamer is only marginally stable in the absence of the A subunit; thus, when used as an immunogen, is not able to raise specific Abs against conformational epitopes that are located primarily at the interfaces between monomers of the pentamer. In contrast, the fusion to BLS strongly increases the stability of Stx2B, allowing the development of Abs against the native conformation of the pentamer.

More significantly, the Abs induced by the chimera showed a similar neutralizing capacity against wild-type Stx2, its variants, and rStx1. It was demonstrated that all Gb3Cer binding sites in this family of toxins are located on the same face of the B pentamer, opposite the A subunit. Two of the three binding sites are formed by residues contributed by neighboring monomers and require correct assembly of the pentamer (45). Thus, the serum's capacity to neutralize different Stx family members primarily would be due to Abs recognizing these binding sites that are conserved in all members of the Stx family (49), which are only present when the B subunit adopts the spatial pentameric conformation (50). This fact is of great importance for prophylaxis or therapeutics of HUS, because Abs showing broad reactivity against Gb3Cer binding sites should be highly effective at preventing the damage caused by the entire Stx family.

Effective vaccines rely on two key factors: an Ag against which adaptive immune responses are generated and an immune stimulus or adjuvant to signal the innate immune system to potentiate the Ag-specific response (51). Highly purified Ags offer potential advantages over traditional vaccines, including their safety and the capacity to elicit highly specific immune responses (52); however, in general, they need to be coadministered with immunostimulant substances (adjuvants) because they are poorly immunogenic (51, 53, 54). In the current study, immunization with BLS-Stx2B chimera formulated in FA was the most effective regimen to induce high titers of specific anti-Stx2B Abs. However, because FA is only suitable for experimental approaches, we tested the immune response and protection induced by the chimera formulated in AH and without exogenous adjuvant. Interestingly, all BLS-Stx2B–immunization regimens, even in the absence of adjuvant, induced a clear protection against the toxin in both in vitro and ex vivo experiments, and all mice vaccinated with the BLS-Stx2B chimera were protected against rStx2 challenge, despite the low ELISA Ab titers observed in some cases. Most importantly, sera from immunized mice also protected mice during a relevant model of EHEC infection, demonstrating that the transferred Abs were capable of neutralizing the toxin as it is delivered by EHEC. In fact, mice receiving immune sera failed to exhibit any of the hallmarks of an EHEC infection (e.g., physical signs of illness, renal disease, neutrophilia, and death). Furthermore, the fact that immune sera reduced EHEC colonization in the intestine suggests that anti-Stx2B Abs may have the ability to neutralize Stx2 locally, because accumulating evidence suggests that Stx2 improves EHEC colonization in mice and cattle (55–57). These results encouraged us to propose that this immunogen could be used as a vaccine against HUS.

In line with previous data (58, 59), we found that the DNA–protein prime-boost regimen resulted in a long-lasting production of anti-Stx2B–specific Abs with neutralizing capacity. In fact, 9 mo after the last immunization, mice vaccinated with the DNA–protein prime-boost regimen showed specific Ab ELISA titers that were similar to their highest values, whereas sera titers from mice vaccinated with FA decreased to 25% of their maximum values. It is important to highlight that all vaccinated mice remained healthy

for 11 mo and were protected even after injection of rStx2 at 3 LD_{100} (10 mo after the last immunization).

In conclusion, considering that Stx2 is the pathogenic factor associated with HUS development, our results demonstrate that BLS-Stx2B should be a useful candidate for the development of subunit vaccines against HUS or for the development of therapeutic anti-Stx–neutralizing Abs to be used during future outbreaks with EHEC or new strains carrying *Stx* genes.

Acknowledgments

We thank Hector Costa and Gabriela Camerano for excellent technical assistance.

Disclosures

The authors have no financial conflicts of interest.

References

1. Kaper, J. B., J. P. Nataro, and H. L. Mobley. 2004. Pathogenic *Escherichia coli*. *Nat. Rev. Microbiol.* 2: 123–140.
2. Karmali, M. A. 1989. Infection by verocytotoxin-producing *Escherichia coli*. *Clin. Microbiol. Rev.* 2: 15–38.
3. Caprioli, A., S. Morabito, H. Brugère, and E. Oswald. 2005. Enterohaemorrhagic *Escherichia coli*: emerging issues on virulence and modes of transmission. *Vet. Res.* 36: 289–311.
4. Griffin, P. M., and R. V. Tauxe. 1991. The epidemiology of infections caused by *Escherichia coli* O157:H7, other enterohemorrhagic *E. coli*, and the associated hemolytic uremic syndrome. *Epidemiol. Rev.* 13: 60–98.
5. López, E. L., V. Prado-Jiménez, M. O'Ryan-Gallardo, and M. M. Contrini. 2000. *Shigella* and Shiga toxin-producing *Escherichia coli* causing bloody diarrhea in Latin America. *Infect. Dis. Clin. North Am.* 14: 41–65, viii.
6. Rivas, M., E. Miliwebsky, I. Chinen, N. Deza, and G. A. Leotta. 2006. [The epidemiology of hemolytic uremic syndrome in Argentina. Diagnosis of the etiologic agent, reservoirs and routes of transmission]. *Medicina (B. Aires)* 66(Suppl. 3): 27–32.
7. Noël, J. M., and E. C. Boedeker. 1997. Enterohemorrhagic *Escherichia coli*: a family of emerging pathogens. *Dig. Dis.* 15: 67–91.
8. O'Brien, A. D., V. L. Tesh, A. Donohue-Rolfe, M. P. Jackson, S. Olsnes, K. Sandvig, A. A. Lindberg, and G. T. Keusch. 1992. Shiga toxin: biochemistry, genetics, mode of action, and role in pathogenesis. *Curr. Top. Microbiol. Immunol.* 180: 65–94.
9. Donohue-Rolfe, A., D. W. Acheson, and G. T. Keusch. 1991. Shiga toxin: purification, structure, and function. *Rev. Infect. Dis.* 13(Suppl. 4): S293–S297.
10. Lingwood, C. A. 1996. Role of verotoxin receptors in pathogenesis. *Trends Microbiol.* 4: 147–153.
11. Friedrich, A. W., M. Bielaszewska, W. L. Zhang, M. Pulz, T. Kuczius, A. Ammon, and H. Karch. 2002. *Escherichia coli* harboring Shiga toxin 2 gene variants: frequency and association with clinical symptoms. *J. Infect. Dis.* 185: 74–84.
12. Rüssmann, H., H. Schmidt, J. Heesemann, A. Caprioli, and H. Karch. 1994. Variants of Shiga-like toxin II constitute a major toxin component in *Escherichia coli* O157 strains from patients with haemolytic uraemic syndrome. *J. Med. Microbiol.* 40: 338–343.
13. Beddoe, T., A. W. Paton, J. Le Nours, J. Rossjohn, and J. C. Paton. 2010. Structure, biological functions and applications of the AB5 toxins. *Trends Biochem. Sci.* 35: 411–418.
14. Johannes, L., and W. Römer. 2010. Shiga toxins—from cell biology to biomedical applications. *Nat. Rev. Microbiol.* 8: 105–116.
15. Smith, M. J., L. D. Teel, H. M. Carvalho, A. R. Melton-Celsa, and A. D. O'Brien. 2006. Development of a hybrid Shiga holotoxoid vaccine to elicit heterologous protection against Shiga toxins types 1 and 2. *Vaccine* 24: 4122–4129.
16. Wen, S. X., L. D. Teel, N. A. Judge, and A. D. O'Brien. 2006. Genetic toxoids of Shiga toxin types 1 and 2 protect mice against homologous but not heterologous toxin challenge. *Vaccine* 24: 1142–1148.
17. Tsuji, T., T. Shimizu, K. Sasaki, Y. Shimizu, K. Tsukamoto, H. Arimitsu, S. Ochi, S. Sugiyama, K. Taniguchi, P. Neri, and H. Mori. 2008. Protection of mice from Shiga toxin-2 toxemia by mucosal vaccine of Shiga toxin 2B-His with *Escherichia coli* enterotoxin. *Vaccine* 26: 469–476.
18. Bentancor, L. V., M. Bilen, R. J. Brando, M. V. Ramos, L. C. Ferreira, P. D. Ghiringhelli, and M. S. Palermo. 2009. A DNA vaccine encoding the enterohemorragic *Escherichia coli* Shiga-like toxin 2 A2 and B subunits confers protective immunity to Shiga toxin challenge in the murine model. *Clin. Vaccine Immunol.* 16: 712–718.
19. Marcato, P., G. Mulvey, R. J. Read, K. Vander Helm, P. N. Nation, and G. D. Armstrong. 2001. Immunoprophylactic potential of cloned Shiga toxin 2 B subunit. *J. Infect. Dis.* 183: 435–443.
20. Bachmann, M. F., U. H. Rohrer, T. M. Kündig, K. Bürki, H. Hengartner, and R. M. Zinkernagel. 1993. The influence of antigen organization on B cell responsiveness. *Science* 262: 1448–1451.
21. Kitova, E. N., G. L. Mulvey, T. Dingle, I. Sinelnikov, S. Wee, T. P. Griener, G. D. Armstrong, and J. S. Klassen. 2009. Assembly and stability of the shiga toxins investigated by electrospray ionization mass spectrometry. *Biochemistry* 48: 5365–5374.
22. Velikovsky, C. A., F. A. Goldbaum, J. Cassataro, S. Estein, R. A. Bowden, L. Bruno, C. A. Fossati, and G. H. Giambartolomei. 2003. *Brucella* lumazine synthase elicits a mixed Th1-Th2 immune response and reduces infection in mice challenged with *Brucella abortus* 544 independently of the adjuvant formulation used. *Infect. Immun.* 71: 5750–5755.
23. Zylberman, V., P. O. Craig, S. Klinke, B. C. Braden, A. Cauerhff, and F. A. Goldbaum. 2004. High order quaternary arrangement confers increased structural stability to *Brucella* sp. lumazine synthase. *J. Biol. Chem.* 279: 8093–8101.
24. Bellido, D., P. O. Craig, M. V. Mozgovoj, D. D. Gonzalez, A. Wigdorovitz, F. A. Goldbaum, and M. J. Dus Santos. 2009. *Brucella* spp. lumazine synthase as a bovine rotavirus antigen delivery system. *Vaccine* 27: 136–145.
25. Cassataro, J., K. A. Pasquevich, S. M. Estein, D. A. Laplagne, C. A. Velikovsky, S. de la Barrera, R. Bowden, C. A. Fossati, G. H. Giambartolomei, and F. A. Goldbaum. 2007. A recombinant subunit vaccine based on the insertion of 27 amino acids from Omp31 to the N-terminus of BLS induced a similar degree of protection against *B. ovis* than Rev.1 vaccination. *Vaccine* 25: 4437–4446.
26. Laplagne, D. A., V. Zylberman, N. Ainciart, M. W. Steward, E. Sciutto, C. A. Fossati, and F. A. Goldbaum. 2004. Engineering of a polymeric bacterial protein as a scaffold for the multiple display of peptides. *Proteins* 57: 820–828.
27. Creydt, V. P., M. F. Miyakawa, F. Martín, E. Zotta, C. Silberstein, and C. Ibarra. 2004. The Shiga toxin 2 B subunit inhibits net fluid absorption in human colon and elicits fluid accumulation in rat colon loops. *Braz. J. Med. Biol. Res.* 37: 799–808.
28. Capozzo, A. V., V. Pistone Creydt, G. Dran, G. Fernández, S. Gómez L. V. Bentancor, C. Rubel, C. Ibarra, M. Isturiz, and M. S. Palermo. 2003. Development of DNA vaccines against hemolytic-uremic syndrome in a murine model. *Infect. Immun.* 71: 3971–3978.
29. Fernández-Brando, R. J., L. V. Bentancor, M. P. Mejías, M. V. Ramos, A. Exeni, C. Exeni, Mdel. C. Laso, R. Exeni, M. A. Isturiz, and M. S. Palermo. 2011. Antibody response to Shiga toxins in Argentinean children with enteropathic hemolytic uremic syndrome at acute and long-term follow-up periods. *PLoS ONE* 6: e19136.
30. Ishikawa, S., K. Kawahara, Y. Kagami, Y. Isshiki, A. Kaneko, H. Matsui, N. Okada, and H. Danbara. 2003. Protection against Shiga toxin 1 challenge by immunization of mice with purified mutant Shiga toxin 1. *Infect. Immun.* 71: 3235–3239.
31. Bentancor, L. V., M. F. Bilen, M. P. Mejías, R. J. Fernández-Brando, C. A. Panek, M. V. Ramos, G. C. Fernández, M. Isturiz, P. D. Ghiringhelli, and M. S. Palermo. 2013. Functional capacity of Shiga-toxin promoter sequences in eukaryotic cells. *PLoS ONE* 8: e57128.
32. Ashkenazi, S., and T. G. Cleary. 1989. Rapid method to detect shiga toxin and shiga-like toxin I based on binding to globotriosyl ceramide (Gb3), their natural receptor. *J. Clin. Microbiol.* 27: 1145–1150.
33. Lasaro, M. A., C. Mathias-Santos, J. F. Rodrigues, and L. C. Ferreira. 2009. Functional and immunological characterization of a natural polymorphic variant of a heat-labile toxin (LT-I) produced by enterotoxigenic *Escherichia coli* (ETEC). *FEMS Immunol. Med. Microbiol.* 55: 93–99.
34. Brando, R. J., E. Miliwebsky, L. Bentancor, N. Deza, A. Baschkier, M. V. Ramos, G. C. Fernández, R. Meiss, M. Rivas, and M. S. Palermo. 2008. Renal damage and death in weaned mice after oral infection with Shiga toxin 2-producing *Escherichia coli* strains. *Clin. Exp. Immunol.* 153: 297–306.
35. Nagano, K., K. Taguchi, T. Hara, S. Yokoyama, K. Kawada, and H. Mori. 2003. Adhesion and colonization of enterohemorrhagic *Escherichia coli* O157:H7 in cecum of mice. *Microbiol. Immunol.* 47: 125–132.
36. Fernandez, M. I., A. Thuizat, T. Pedron, M. Neutra, A. Phalipon, and P. J. Sansonetti. 2003. A newborn mouse model for the study of intestinal pathogenesis of shigellosis. *Cell. Microbiol.* 5: 481–491.
37. Leotta, G. A., I. Chinen, S. Epszteyn, E. Miliwebsky, I. C. Melamed, M. Motter, M. Ferrer, E. Marey, and M. Rivas. 2005. [Validation of a multiplex PCR for detection of Shiga toxin-producing *Escherichia coli*]. *Rev. Argent. Microbiol.* 37: 1–10.
38. Ziebell, K. A., S. C. Read, R. P. Johnson, and C. L. Gyles. 2002. Evaluation of PCR and PCR-RFLP protocols for identifying Shiga toxins. *Res. Microbiol.* 153: 289–300.
39. Paton, A. W., and J. C. Paton. 1998. Detection and characterization of Shiga toxigenic *Escherichia coli* by using multiplex PCR assays for stx1, stx2, eaeA, enterohemorrhagic *E. coli* hlyA, rfbO111, and rfbO157. *J. Clin. Microbiol.* 36: 598–602.
40. Craig, P. O., V. Alzogaray, and F. A. Goldbaum. 2012. Polymeric Display of Proteins through High Affinity Leucine Zipper Peptide Adaptors. *Biomacromolecules* 13: 1112–1121.
41. Craig, P. O., P. M. Berguer, N. Ainciart, V. Zylberman, M. G. Thomas, L. J. Martinez Tosar, A. Bulloj, G. L. Boccaccio, and F. A. Goldbaum. 2005. Multiple display of a protein domain on a bacterial polymeric scaffold. *Proteins* 61: 1089–1100.
42. Lim, Y. S., B. Y. Kang, E. J. Kim, S. H. Kim, S. Y. Hwang, and T. S. Kim. 1998. Potentiation of antigen-specific, Th1 immune responses by multiple DNA vaccination with an ovalbumin/interferon-gamma hybrid construct. *Immunology* 94: 135–141.
43. Fernandez-Brando, R. J., E. Miliwebsky, M. P. Mejías, A. Baschkier, C. A. Panek, M. J. Abrey-Recalde, G. Cabrera, M. V. Ramos, M. Rivas, and M. S. Palermo. 2012. Shiga toxin-producing *Escherichia coli* O157 : H7 shows an increased pathogenicity in mice after the passage through the gastrointestinal tract of the same host. *J. Med. Microbiol.* 61: 852–859.
44. Cai, K., X. Gao, T. Li, Q. Wang, X. Hou, W. Tu, L. Xiao, M. Tian, Y. Liu, and H. Wang. 2011. Enhanced immunogenicity of a novel Stx2Am-Stx1B fusion protein in a mice model of enterohemorrhagic *Escherichia coli* O157:H7 infection. *Vaccine* 29: 946–952.
45. Ling, H., A. Boodhoo, B. Hazes, M. D. Cummings, G. D. Armstrong, J. L. Brunton, and R. J. Read. 1998. Structure of the shiga-like toxin I B-

pentamer complexed with an analogue of its receptor Gb3. *Biochemistry* 37: 1777–1788.
46. Beutin, L., J. A. Hammerl, E. Strauch, J. Reetz, R. Dieckmann, Y. Kelner-Burgos, A. Martin, A. Miko, N. A. Strockbine, B. A. Lindstedt, et al. 2012. Spread of a distinct Stx2-encoding phage prototype among *Escherichia coli* O104:H4 strains from outbreaks in Germany, Norway, and Georgia. *J. Virol.* 86: 10444–10455.
47. Scheutz, F., E. M. Nielsen, J. Frimodt-Møller, N. Boisen, S. Morabito, R. Tozzoli, J. P. Nataro, and A. Caprioli. 2011. Characteristics of the enteroaggregative Shiga toxin/verotoxin-producing *Escherichia coli* O104:H4 strain causing the outbreak of haemolytic uraemic syndrome in Germany, May to June 2011. *Euro Surveill.* 16: 16.
48. Berguer, P. M., J. Mundiñano, I. Piazzon, and F. A. Goldbaum. 2006. A polymeric bacterial protein activates dendritic cells via TLR4. *J. Immunol.* 176: 2366–2372.
49. Ling, H., N. S. Pannu, A. Boodhoo, G. D. Armstrong, C. G. Clark, J. L. Brunton, and R. J. Read. 2000. A mutant Shiga-like toxin IIe bound to its receptor Gb(3): structure of a group II Shiga-like toxin with altered binding specificity. *Structure* 8: 253–264.
50. Fraser, M. E., M. Fujinaga, M. M. Cherney, A. R. Melton-Celsa, E. M. Twiddy, A. D. O'Brien, and M. N. James. 2004. Structure of shiga toxin type 2 (Stx2) from *Escherichia coli* O157:H7. *J. Biol. Chem.* 279: 27511–27517.
51. Coffman, R. L., A. Sher, and R. A. Seder. 2010. Vaccine adjuvants: putting innate immunity to work. *Immunity* 33: 492–503.
52. Demotz, S., C. Moulon, M. A. Roggero, N. Fasel, and S. Masina. 2001. Native-like, long synthetic peptides as components of sub-unit vaccines: practical and theoretical considerations for their use in humans. *Mol. Immunol.* 38: 415–422.
53. Lima, K. M., S. A. dos Santos, J. M. Rodrigues, Jr., and C. L. Silva. 2004. Vaccine adjuvant: it makes the difference. *Vaccine* 22: 2374–2379.
54. Reed, S. G., S. Bertholet, R. N. Coler, and M. Friede. 2009. New horizons in adjuvants for vaccine development. *Trends Immunol.* 30: 23–32.
55. Robinson, C. M., J. F. Sinclair, M. J. Smith, and A. D. O'Brien. 2006. Shiga toxin of enterohemorrhagic *Escherichia coli* type O157:H7 promotes intestinal colonization. *Proc. Natl. Acad. Sci. USA* 103: 9667–9672.
56. Mohawk, K. L., A. R. Melton-Celsa, C. M. Robinson, and A. D. O'Brien. 2010. Neutralizing antibodies to Shiga toxin type 2 (Stx2) reduce colonization of mice by Stx2-expressing *Escherichia coli* O157:H7. *Vaccine* 28: 4777–4785.
57. Hoey, D. E., C. Currie, R. W. Else, A. Nutikka, C. A. Lingwood, D. L. Gally, and D. G. Smith. 2002. Expression of receptors for verotoxin 1 from *Escherichia coli* O157 on bovine intestinal epithelium. *J. Med. Microbiol.* 51: 143–149.
58. Law, M., R. M. Cardoso, I. A. Wilson, and D. R. Burton. 2007. Antigenic and immunogenic study of membrane-proximal external region-grafted gp120 antigens by a DNA prime-protein boost immunization strategy. *J. Virol.* 81: 4272–4285.
59. Davtyan, H., M. Mkrtichyan, N. Movsesyan, I. Petrushina, G. Mamikonyan, D. H. Cribbs, M. G. Agadjanyan, and A. Ghochikyan. 2010. DNA prime-protein boost increased the titer, avidity and persistence of anti-Abeta antibodies in wild-type mice. *Gene Ther.* 17: 261–271.